

Regulation of Cell pH by Ambient Bicarbonate, Carbon Dioxide Tension, and pH in the Rabbit Proximal Convoluted Tubule

Reto Krapf, Christine A. Berry, Robert J. Alpern, and Floyd C. Rector, Jr.

Department of Medicine, Cardiovascular Research Institute, University of California, San Francisco, California 94143-0532

Abstract

To study the regulation of cell pH by ambient pH, carbon dioxide tension (PCO_2), and bicarbonate (HCO_3^-), cell pH was measured in the isolated, *in vitro* microperfused rabbit proximal convoluted tubule using the fluorescent dye (2',7')-bis-(carboxyethyl)-(5,6)-carboxyfluorescein. For the same changes in external pH, changes in $[\text{HCO}_3^-]$ and PCO_2 affected cell pH similarly ($[\text{HCO}_3^-]$: $\text{pH}_i/\text{pH}_e = 0.67$, PCO_2 : $\text{pH}_i/\text{pH}_e = 0.64$, NS). Isohydic changes in extracellular $[\text{HCO}_3^-]$ and PCO_2 did not change cell pH significantly. Changes in peritubular $[\text{HCO}_3^-]$ elicited larger changes in cell pH than changes in luminal $[\text{HCO}_3^-]$, which were enhanced by peritubular 4-acetamido-4'-isothiocyanostilbene-2,2'-disulfonate (SITS). The cell pH defense against acute increases and decreases in PCO_2 was inhibited by sodium, but not by chloride removal. Peritubular SITS inhibited the cell pH defense against increases and decreases of PCO_2 , whereas luminal amiloride inhibited cell pH defense against increases in PCO_2 .

Conclusions: (a) Steady-state cell pH changes in response to changes in extracellular $[\text{HCO}_3^-]$ and PCO_2 are quantitatively similar for a given change in extracellular pH; (b) the rate of the basolateral $\text{Na}/(\text{HCO}_3)_3$ cotransporter is a more important determinant of cell pH than the rate of the apical membrane mechanism(s); (c) cell pH defense against acute changes in PCO_2 depends on the basolateral $\text{Na}/(\text{HCO}_3)_3$ cotransporter (acid and alkaline loads) and the luminal Na/H antiporter (acid loads).

Introduction

Systemic acid-base disturbances have profound effects on transepithelial proton secretion and bicarbonate reabsorption in the mammalian proximal convoluted tubule (PCT).¹ Among others, the following three factors have been shown to be important: (a) changes in luminal pH and $[\text{HCO}_3^-]$, (b) changes in peritubular pH and $[\text{HCO}_3^-]$, and (c) changes in ambient carbon dioxide tension (PCO_2) (1).

Address correspondence and reprint requests to Dr. Krapf, Box 0532, 1065 HSE, Division of Nephrology, University of California, San Francisco, CA 94143-0532.

Received for publication 28 May 1987 and in revised form 5 August 1987.

1. Abbreviations used in this paper: BCECF, (2',7')-bis-(carboxyethyl)-5,6-carboxyfluorescein; HCO_3^- , bicarbonate; PCO_2 , carbon dioxide tension; PCT, proximal convoluted tubule; SITS, 4-acetamido-4'-isothiocyanostilbene-2,2'-disulfonate.

J. Clin. Invest.

© The American Society for Clinical Investigation, Inc.

0021-9738/88/02/0381/09 \$2.00

Volume 81, February 1988, 381-389

Over a wide range (5–40 mM), incremental increases in luminal $[\text{HCO}_3^-]$ lead to a linear increase in HCO_3^- reabsorption in the late PCT (2–5). The changes in luminal $[\text{HCO}_3^-]$ and pH affect HCO_3^- reabsorption (or proton secretion) at least in part by changing the rate of the apical Na/H antiporter (6). Increases in peritubular $[\text{HCO}_3^-]$ inhibit and decreases in peritubular bicarbonate concentration stimulate net HCO_3^- reabsorption (4, 5, 7–10). Since peritubular pH does not affect the small HCO_3^- permeability (2), changes in peritubular $[\text{HCO}_3^-]$ exert their influence on transcellular H/HCO_3^- transport. The recently described $\text{Na}/(\text{HCO}_3)_3$ symporter on the basolateral membrane of the proximal tubule (12–19) is an important mechanism by which changes in peritubular pH and $[\text{HCO}_3^-]$ can affect HCO_3^- reabsorption. Finally, increases in PCO_2 have been shown to stimulate and decreases in PCO_2 to inhibit HCO_3^- reabsorption (5, 11, 20–22). The cellular mechanisms of these effects, however, are unknown.

To affect transcellular proton secretion or HCO_3^- reabsorption, changes in luminal $[\text{HCO}_3^-]$ and pH have to change the rate of the basolateral base exit to a similar degree as they change the rate of apical proton secretion in the steady state. Similarly, changes in peritubular $[\text{HCO}_3^-]$ and pH have to affect the rate of apical proton secretion secondarily. One important mechanism by which these secondary changes might occur is a change in cell pH. Changes in PCO_2 are expected to change luminal and peritubular pH equally. Thus, the change in cell pH (which is expected to differ from the change in extracellular pH due to differences in buffer composition) might be the important determinant that regulates HCO_3^- reabsorption when ambient PCO_2 changes. Since cell pH changes are important mediators of HCO_3^- reabsorption, the independent and interdependent roles of changes in ambient $[\text{HCO}_3^-]$ and PCO_2 in regulation of cell pH need to be analyzed in order to understand the behavior of the proximal tubule in acid-base disturbances.

The purposes of these studies therefore were (a) to compare the cell pH response to changes in ambient $[\text{HCO}_3^-]$ and PCO_2 , (b) to examine the effects of isohydric changes in $[\text{HCO}_3^-]$ and PCO_2 ; (c) to analyze the relative importance of luminal and basolateral $\text{HCO}_3^-/\text{OH}/\text{H}$ transporters in the cell pH response to changes in $[\text{HCO}_3^-]$, and (d) to characterize the mechanisms involved in the cell pH response to acute changes in ambient PCO_2 .

For the performance of these studies we chose the technique of *in vitro* microperfusion of rabbit PCT, which permits adequate control of the acid-base parameters in luminal and peritubular perfusates. Cell pH was measured microfluorometrically using the pH-sensitive dye (2',7')-bis-(carboxyethyl)-5,6-carboxyfluorescein (BCECF). The results demonstrate that: (a) changes in cell pH in response to changes in extracellular $[\text{HCO}_3^-]$ and PCO_2 are quantitatively similar for a given change in extracellular pH; (b) the rate of the basolateral $\text{HCO}_3^-/\text{OH}/\text{H}$ transporters is a quantitatively more important

determinant of cell pH than is the rate of the apical HCO₃/OH/H transporters; and (c) cell pH defense in response to acute changes in ambient PCO₂ is primarily accomplished by the action of the apical Na/H antiporter (recovery from acid load) and the basolateral Na/(HCO₃)₃ cotransporter (recovery from acid and alkaline loads), whereas chloride-dependent transporters do not contribute to a detectable degree.

Methods

Isolated segments of rabbit PCT were dissected and perfused in vitro as previously described (23). Briefly, kidneys from New Zealand white rabbits, killed by decapitation, were quickly removed and cut into thin (~ 1 mm) coronal slices. Cortical PCT (S1 and S2 segments) were dissected in the cooled (4°C) control solution of the respective experiment (Table I). Late PCT, as defined by their attachment to straight tubules, were not used. The tubules were transferred into a bath chamber with a volume of 150 μl. Bath fluid was exchanged continuously at about 10 ml/min, thus permitting a complete bath fluid exchange within ~ 1 s, as reported previously (17). Bath pH was continuously monitored by placing a commercial, flexible pH electrode into the bath (MI 21960, Microelectrodes, Inc., Londonderry, NH). The actual bath pH values varied by ±0.02 pH units from the desired values (pH meter 145, Corning Medical, Medfield, MA). Bath solutions were preheated to 38°C and equilibrated with the appropriate gasses to obtain the desired PCO₂ (see Table I). Just before the bath chamber, a specially designed heater (glass tubing surrounded by a coiled high-resistance heating wire) was placed in line and connected to a power supply. With this setup, bath temperature could be held constant at 38±0.5°C. The fluid in the perfusing pipette was exchanged continuously at a rate of 2 ml/min through hydrostatic pressure and a constantly open efflux valve. The time lag between the change from a control to an experimental luminal solution and its appearance at the most proximal portions of the perfused tubule was ~ 10 s. This was

repeatedly confirmed by recording the fluorescence signal at the tip of the perfusing pipette when an exchange was performed to a solution containing a fluorescent dye (BCECF salt). At a perfusion rate of 10 ml/min the bath lag time was 4 s. Thus, a coordinated fluid exchange (bath fluid changed 6 s after luminal fluid exchange) permitted synchronization of luminal and bath fluid exchanges.

The perfusion solutions used in this study are listed in Table I. 4-Acetamido-4'-isothiocyanostilbene-2,2'-disulfonate (SITS) was obtained from International Chemical and Nuclear (Cleveland, OH). Amiloride was purchased from Sigma Chemical Co. (St. Louis, MO).

Cell pH measurement. After allowing the tubule to equilibrate at 38°C for 15 min in the control solution, the tubules were loaded with the acetoxymethyl (AM) derivative of BCECF (BCECF-AM, Molecular Probes, Eugene, OR) from the bath in a concentration of 4 μM, as described previously (17). The tubules were loaded for 5–8 min. The first fluorescence measurements were made not earlier than 5 min after loading because intracellular cleavage of the ester bonds of BCECF-AM constitutes a small acid load to the cell. When two protocols were performed using the same tubule, the tubules were allowed to equilibrate with the new control solution without light exposure for 5 min.

Fluorescence measurements were made with an inverted fluorescent microscope (Fluovert, Leitz-Wetzlar) using a × 25 objective. An adjustable measuring diaphragm was appropriately placed over the tubule and opened to about 40–70 μm square. The tubule length exposed to the bath fluid was 300–400 μm. Background fluorescence was measured before loading the tubule with the dye. After this measurement, the measuring diaphragm was left in the same place for the entire experiment. The signal-to-background ratio at the end of the experiments varied from about 25 to 100 at 500 nm and from about 15 to 65 at 450 nm excitation.

BCECF has a peak excitation at 504 nm that is pH sensitive and an isosbestic point at 436 nm, where fluorescence is independent of pH. Peak emission is at 526 nm (14). Fluorescence was measured as previously described (14, 17), alternately at 500- and 450-nm excitation and at an emission wavelength of 530 nm (interference filters, Corion Corp., Holliston, MA). After correcting all measurements for back-

Table I. Perfusion Solutions

| | Solution | | | | | | | | | |
|-------------------------------|-------------------|-------|-------|--------|------|------|--------|------|-------|-------|
| | 1* | 2 | 3 | 4 | 5 | 6 | 7 | 8 | 9 | 10 |
| | <i>mmol/liter</i> | | | | | | | | | |
| Na ⁺ | 147 | 147 | 147 | 147 | 147 | 147 | 147 | 147 | | 147 |
| K ⁺ | 5 | 5 | 5 | 5 | 5 | 5 | 5 | 5 | 5 | 5 |
| Ca ²⁺ | 1.8 | 1.8 | 1.8 | 1.8 | 1.8 | 1.8 | 1.8 | 1.8 | 1.8 | 9.4 |
| Mg ²⁺ | 1 | 1 | 1 | 1 | 1 | 1 | 1 | 1 | 1 | 1 |
| Choline ⁺ | | | | | | | | | 147 | |
| NH ₄ ⁺ | | | | | | | | | | |
| Cl ⁻ | 128.6 | 141.1 | 144.1 | 147.35 | 93.6 | 58.6 | 147.35 | 91.1 | 128.6 | |
| HCO ₃ ⁻ | 25 | 12.5 | 9.5 | 6.25 | 60 | 95 | 6.25 | 62.5 | 25 | 25 |
| HPO ₄ ⁻ | 1 | 1 | 1 | 1 | 1 | 1 | 1 | 1 | 1 | 1 |
| SO ₄ ⁻ | 1 | 1 | 1 | 1 | 1 | 1 | 1 | 1 | 1 | 1 |
| Gluconate ⁻ | | | | | | | | | | 134.4 |
| Glucose | 5 | 5 | 5 | 5 | 5 | 5 | 5 | 5 | 5 | 5 |
| Alanine | 5 | 5 | 5 | 5 | 5 | 5 | 5 | 5 | 5 | 5 |
| Urea | 5 | 5 | 5 | 5 | 5 | 5 | 5 | 5 | 5 | 5 |
| CO ₂ (mmHg) | 40 | 40 | 40 | 40 | 40 | 40 | 10 | 105 | 40 | 40 |
| pH | 7.4 | 7.12 | 7.0 | 6.82 | 7.8 | 8.0 | 7.4 | 7.4 | 7.4 | 7.4 |

* For protocols using different PCO₂ values solution 1 was used and bubbled with 1.1% (PCO₂ 10 mmHg), 2.5% CO₂ (PCO₂ 16 mmHg), 5% (PCO₂ 40 mmHg), 10% (80 mmHg), and 14% (105 mmHg) CO₂ gas.

ground, the means of two 500-nm excitation measurements were divided by the 450-nm excitation measurement between them, thereby yielding the fluorescence excitation ratio (F_{500}/F_{450}). For each determination, these measurements were performed twice and their mean used to estimate cell pH. The use of the ratio provides a measurement that is unaffected by changes in dye concentration (24). To convert fluorescence excitation ratios to an apparent cell pH value, results of our previously reported intracellular calibration were used (17). In brief, tubules were calibrated by perfusion with well-buffered solutions (25 mM Hepes, 33 mM phosphate) containing nigericin (a K/H antiporter, 7 μ M) and 66 mM K.

In some studies, the rate of cell pH change was calculated, as described previously (17). During a fluid exchange, fluorescence was followed at 500-nm excitation on a chart recorder (LS 52, Linseis Inc., Princeton Junction, NJ). The slope of a line drawn tangent to the initial deflection (dF_{500}/dt) defined the initial rate of change in 500-nm fluorescence. Because fluorescence with 450-nm excitation is pH insensitive (14), it can be considered constant. By measuring fluorescence at 450 nm before and after the fluid exchange, the actual value of the 450-nm excitation at the time of the initial deflection of 500 nm was determined by interpolation. The rate of change in the fluorescence excitation ratio [$d(F_{500}/F_{450})/dt$] was then calculated using the formula: $d(F_{500}/F_{450})/dt = [d(F_{500})/dt]/F_{450}$.

Because the slope of the line of our intracellular calibration curve (17) is 1.13 pH unit⁻¹, the rate of cell pH change was calculated according to the formula: $dpH_i/dt = [(dF_{500}/dt)/F_{450}]/1.13$.

The data were analyzed using the paired *t* test. A *P* value of < 0.05 was accepted for statistical significance. Results are reported as means \pm standard error.

Results

Effect of ambient $[HCO_3^-]$ and PCO_2 on cell pH. The first set of studies was designed to compare the effects of PCO_2 and $[HCO_3^-]$ on cell pH. Ambient pH was changed either by varying PCO_2 or $[HCO_3^-]$. Tubules were initially perfused symmetrically with 25 mM HCO_3^- and a PCO_2 of 40 mmHg (solution 1, Table I). When the HCO_3^- effect was examined, luminal and

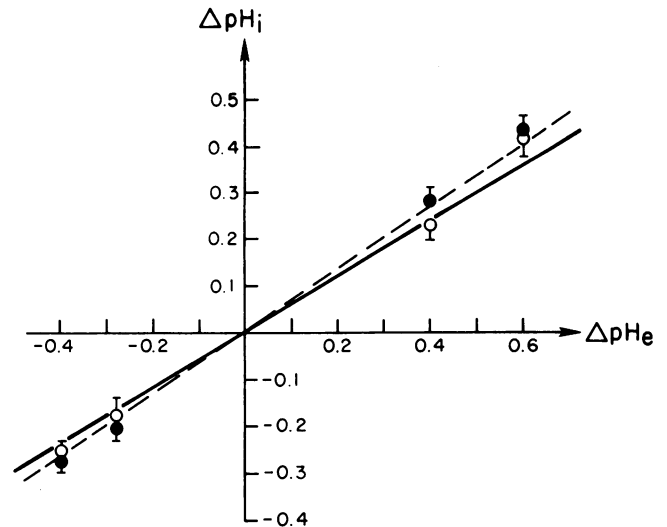


Figure 1. Effects of changes in extracellular pH on cell pH (ΔpH_i) are plotted against changes in extracellular pH (ΔpH_e) for changes in extracellular $[HCO_3^-]$ (●) and ambient PCO_2 (○). The ratio of $\Delta pH_i/\Delta pH_e$ is 0.67 ± 0.05 for changes in extracellular $[HCO_3^-]$, and 0.64 ± 0.03 for changes in ambient PCO_2 (NS).

bath perfusates were changed simultaneously to solutions with a PCO_2 of 40 mmHg containing either 9.5 mM (pH = 7.00), 12.5 mM (pH = 7.12), 60 mM (pH = 7.80), or 95 mM (pH = 8.00) HCO_3^- (solutions 2, 3, 5, and 6, respectively, Table I). When the PCO_2 effect was examined, the bath perfusate was changed to solutions with a $[HCO_3^-]$ of 25 mM and PCO_2 values of 105 mmHg (pH = 7.00), 80 mmHg (pH = 7.12), 16 mmHg (pH = 7.80), and 10 mmHg (pH = 8.00), respectively (solution 1, Table I, bubbled with the appropriate CO_2/O_2 mixtures). The PCO_2 and the HCO_3^- effects for the same pH value were examined in the same tubule in paired experiments. In 50% of the tubules the PCO_2 and in the other 50% the HCO_3^- effect was examined first. The baseline pH values, the calculated initial rate of cell pH change and the mean change in steady-state cell pH induced by changing either ambient $[HCO_3^-]$ or PCO_2 are given in Table II. In each protocol examining a given change in ambient pH, eight tubules were studied. The data show that the rates of cell pH change at the same ambient pH gradient are significantly faster when PCO_2 is changed. In addition, the rates become faster when the magnitude of changes in PCO_2 or $[HCO_3^-]$ is increased.² More importantly, however, the mean change in cell pH is not significantly different when ambient pH is changed either by varying $[HCO_3^-]$ or PCO_2 . The relationship between changes in ambient pH and changes in cell pH is illustrated in Fig. 1. For HCO_3^- -induced pH changes the ratio of change in cell pH to change in ambient pH ($\Delta pH_i/\Delta pH_e$) is 0.67 ± 0.05 and for PCO_2 -induced pH changes $\Delta pH_i/\Delta pH_e$ is 0.64 ± 0.03 (NS).

The above studies suggest that extracellular $[HCO_3^-]$ and PCO_2 have similar effects on steady state cell pH. If so, isohydric changes in the extracellular fluid should have little effect on cell pH. We examined this prediction in the next set of

Table II. Effects of Changes in Ambient $[HCO_3^-]$ and PCO_2 on Cell pH

| Ambient pH | Baseline pH_i | Initial rate of cell pH change dpH_i/dt | ΔpH_i [§] |
|----------------------|-----------------|--|----------------------------|
| 7.4–7.8 | | | |
| PCO_2 40–16 mmHg | 7.33 ± 0.07 | 2.3 ± 0.3 | 0.23 ± 0.03 |
| HCO_3^- 25–60 mM | 7.30 ± 0.05 | $1.5 \pm 0.4^*$ | 0.28 ± 0.03 (NS) |
| 7.4–8.0 | | | |
| PCO_2 40–10 mmHg | 7.32 ± 0.05 | 5.2 ± 1.4 | 0.42 ± 0.04 |
| HCO_3^- 25–95 mM | 7.34 ± 0.05 | $1.9 \pm 0.2^\ddagger$ | 0.43 ± 0.03 (NS) |
| 7.4–7.12 | | | |
| PCO_2 40–80 mmHg | 7.27 ± 0.04 | 2.7 ± 0.2 | 0.18 ± 0.04 |
| HCO_3^- 25–12.5 mM | 7.24 ± 0.05 | $1.6 \pm 0.3^*$ | 0.21 ± 0.02 (NS) |
| 7.4–7.0 | | | |
| PCO_2 40–105 mmHg | 7.29 ± 0.04 | 5.7 ± 1.8 | 0.25 ± 0.02 |
| HCO_3^- 25–9.5 mM | 7.31 ± 0.05 | $1.8 \pm 0.4^*$ | 0.27 ± 0.04 (NS) |

* *P* < 0.01 compared with effect of PCO_2 .

† *P* < 0.025 compared with PCO_2 effect.

§ ΔpH_i , mean change in cell pH compared with pre- and postcontrols.

2. In view of the high CO_2 permeability of the proximal tubular cells (25), the initial rates of cell pH changes calculated for changes in PCO_2 might represent underestimates because of limitations by bath fluid exchange time (about 1 s).

studies. In the control period, tubules were perfused with 25 mM HCO_3^- at a PCO_2 of 40 mmHg (solution 1, Table I). In the experimental period, solutions were changed to either 6.25 mM HCO_3^- at a PCO_2 of 10 mmHg or 62.5 mM HCO_3^- at a PCO_2 of 105 mmHg. In all periods, extracellular pH was 7.4. Each experiment was performed in a total of seven tubules. The results of these studies are summarized in Table III. For isohydric changes performed using 6.25 mM HCO_3^- and a PCO_2 of 10 mmHg, the steady-state cell pH was 0.04 ± 0.02 pH units lower than in the control periods (not significantly different from zero) and for isohydric changes using 62.5 mM HCO_3^- and a PCO_2 of 105 mmHg the steady-state cell pH was 0.04 ± 0.03 pH units lower than in the control periods (not significantly different from zero). Thus, these results show that the steady-state cell pH is not significantly different from controls when ambient $[\text{HCO}_3^-]$ and PCO_2 are changed isohydrically. Taken together, the above results demonstrate that extracellular $[\text{HCO}_3^-]$ and PCO_2 have quantitatively similar effects on steady state cell pH.

Effect of luminal and peritubular pH on cell pH. The next set of studies was designed to examine the relative effects of luminal and peritubular pH on cell pH. Studies in the rat PCT suggest that the rate of basolateral $\text{HCO}_3^-/\text{OH}^-/\text{H}^+$ membrane transporter(s) is more sensitive to a given change in ambient pH than is the rate of apical $\text{HCO}_3^-/\text{OH}^-/\text{H}^+$ membrane transporter(s) (26). Experiments comparing the effects on cell pH of changes in luminal versus changes in luminal and peritubular $[\text{HCO}_3^-]$ were performed in the absence and presence of 1 mM bath SITS to inhibit the basolateral $\text{Na}/(\text{HCO}_3^-)_3$ cotransporter (14, 17). Tubules were perfused symmetrically with 25 mM HCO_3^- at a PCO_2 of 40 mmHg (pH = 7.4, solution 1, Table I). In one set of studies, $[\text{HCO}_3^-]$ was lowered to 6.25 mM in the lumen and then in the lumen and bath (PCO_2 constant at 40 mmHg, ambient pH = 6.82, solution 4, Table I). In the same tubule, these studies were repeated in the presence of 1 mM SITS in the bath fluid. In a second set of studies, the technical procedures were the same, but $[\text{HCO}_3^-]$ was raised from 25 to 95 mM at a PCO_2 of 40 mmHg (pH = 8.0, solution 6, Table I). Fig. 2 shows that cell pH decreased by 0.05 ± 0.01 pH units when luminal $[\text{HCO}_3^-]$ was decreased to 6.25 mM and peritubular SITS was absent, but by 0.16 ± 0.03 pH units when peritubular SITS was present ($n = 6$, $P < 0.005$). When $[\text{HCO}_3^-]$ was lowered in lumen and bath, the cells acidified by 0.29 ± 0.05 pH units in the absence, but by only 0.19 ± 0.03 pH units in the presence of bath SITS ($P < 0.05$). Fig. 3 shows that

Table III. Effect of Isohydric Changes in $[\text{HCO}_3^-]$ and PCO_2 on Cell pH

| pH _e * | $[\text{HCO}_3^-]_{\text{L/B}}^{\dagger}$ | PCO_2 | Cell pH | $\overline{\Delta\text{pH}_i}^{\ddagger}$ |
|-------------------|---|----------------|-----------------|---|
| 7.4 | 25 | 40 | 7.29 ± 0.03 | |
| 7.4 | 6.25 | 10 | 7.25 ± 0.03 | -0.04 ± 0.02 (NS) |
| 7.4 | 25 | 40 | 7.32 ± 0.03 | |
| 7.4 | 25 | 40 | 7.28 ± 0.04 | |
| 7.4 | 62.5 | 105 | 7.24 ± 0.03 | -0.04 ± 0.03 (NS) |
| 7.4 | 25 | 40 | 7.29 ± 0.03 | |

* pH_e, external (ambient) pH.

[†] $[\text{HCO}_3^-]_{\text{L,B}}$, HCO_3^- concentration in lumen and bath.

[‡] $\overline{\Delta\text{pH}_i}$, mean change in cell pH compared to pre- and postcontrols.

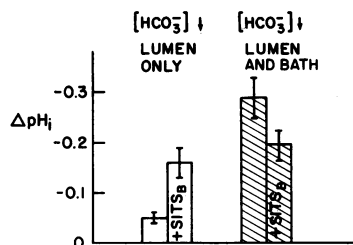


Figure 2. Cell pH response to decreases in luminal and bath $[\text{HCO}_3^-]$ from 25 to 6.25 mM (constant PCO_2 of 40 mmHg). Peritubular SITS increases the cell pH response to a decrease in luminal $[\text{HCO}_3^-]$, but inhibits the cell pH response to a decrease of $[\text{HCO}_3^-]$ in luminal and bath fluids.

the cell pH increased by 0.04 ± 0.01 when luminal $[\text{HCO}_3^-]$ was raised from 25 to 95 mM in the absence of bath SITS. In the presence of SITS, however, the cell pH change increased by 0.10 ± 0.02 pH units ($n = 4$, $P < 0.01$). When $[\text{HCO}_3^-]$ was raised in bath and luminal perfusates the cells alkalinized by 0.25 ± 0.03 pH units in the absence, but by only 0.13 ± 0.02 in the presence of bath SITS ($P < 0.01$). Thus, these studies show that inhibition of basolateral membrane $\text{Na}/(\text{HCO}_3^-)_3$ transport with SITS enhances the response of cell pH to $[\text{HCO}_3^-]$ changes in the luminal fluid. In addition, in the presence of peritubular SITS, the response to a lumen and bath $[\text{HCO}_3^-]$ change is similar to that with a luminal $[\text{HCO}_3^-]$ change alone, confirming that basolateral membrane HCO_3^- permeability is inhibited.

Mechanisms of cell pH response to acute changes in PCO_2 .

To examine the largely unknown mechanisms of cell pH response in the mammalian PCT to acute changes in ambient PCO_2 , we investigated the cell pH response to an acute increase in PCO_2 (40–105 mmHg, external pH change from 7.4 to 7.0, solution 1, Table I) and an acute decrease in PCO_2 (40–10 mmHg, external pH change from 7.4 to 8.0, solution 1, Table I). For each change, the cell pH response was examined in paired studies under the following four conditions: (a) presence and absence of Na in luminal and bath perfusates, (b) presence and absence of Cl in luminal and bath perfusates, (c) absence and presence of 1 mM bath SITS, and (d) absence and presence of 1 mM luminal amiloride. Fig. 4 shows a typical tracing of the changes in fluorescence intensity in response to an acute increase in ambient PCO_2 from 40 to 105 mmHg and serves to illustrate our analysis of the data. The intensity of fluorescence is indicated by the height of the bars. Measurements of 450-nm excitation wavelength are indicated by stars, while all other bars and the recordings during transients are 500-nm excitation measurements. The rapid CO_2 entry decreases 500-nm fluorescence intensity. This initial change (a in Fig. 4) in 500-nm excitation divided by the interpolated 450-nm excitation provides a measure for the initial cell pH change (ΔpH_i initial). The slow recovery phase after this rapid initial

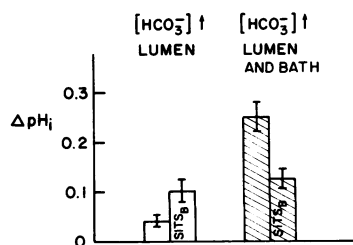


Figure 3. Cell pH response to increases in luminal and bath $[\text{HCO}_3^-]$ from 25 to 95 mM (constant PCO_2 of 40 mmHg). Peritubular SITS enhances the cell pH response to a luminal increase in $[\text{HCO}_3^-]$, but inhibits the cell pH response to increases in both luminal and bath $[\text{HCO}_3^-]$.

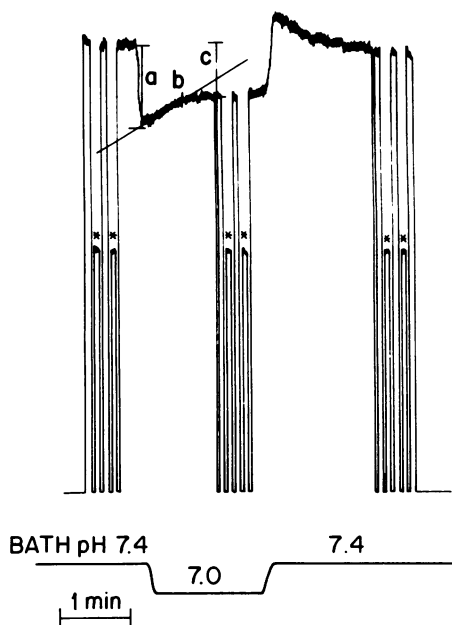


Figure 4. Cell pH response to an acute increase in ambient PCO_2 from 40 to 105 mmHg: original tracing. Fluorescence intensity is indicated by the height of the bars. 450-nm excitation measurements are indicated by asterisks (*), whereas all other bars and recordings during transients represent measurements at 500-nm excitation. The rapid CO_2 entry decreases 500-nm fluorescence intensity. This initial change (a) in 500-nm excitation divided by the interpolated 450-nm excitation provides a measure for the initial change in cell pH (initial acidification). The slow increase (b) in 500-nm fluorescence represents the cell pH defense to the increase in PCO_2 . At c, a new steady state is reached. When PCO_2 is lowered back to 40 mmHg, the fluorescence changes mirror the described alterations in the reverse direction. Bath pH is recorded simultaneously.

change (b in Fig. 4) represents the cell pH defense and its rate was calculated as described in Methods. The change of the 500-nm excitation intensity at the new steady state (c in Fig. 4) divided by the interpolated 450-nm excitation provides a measure for the change in steady-state pH (ΔpH_i steady state). When PCO_2 is brought back to 40 mmHg, fluorescence changes mirror the above described alterations. A rapid in-

crease in 500-nm fluorescence is followed by a slow return to control values. The results of all these studies are compiled in Table IV (raising PCO_2 from 40 to 105 mmHg) and in Table V (lowering PCO_2 from 40 to 10 mmHg). Fig. 5 represents an original tracing illustrating the effect of 1 mM peritubular SITS on cell pH defense to an acute increase in PCO_2 . It can be seen that SITS markedly slowed the rate of cell pH defense. Similarly, as illustrated by the original tracing in Fig. 6, 1 mM luminal amiloride also inhibited the cell pH defense to the same PCO_2 challenge. Fig. 7 provides a summary of the observed rates of cell pH defense under the eight conditions tested. The results are expressed in percentage of the control rate. From this figure it can be concluded, that (a) the cell pH defense to both lowering and increasing PCO_2 is Na dependent; (b) chloride removal has no significant effect on the rate of cell pH defense; (c) inhibition of the basolateral $\text{Na}/(\text{HCO}_3)_3$ transporter by SITS slows the rate of cell pH defense significantly, when PCO_2 is raised or lowered; and (d) inhibition of the apical Na/H antiporter by 1 mM amiloride also inhibits the rate of cell pH defense in response to an increase in PCO_2 , but is without effect when PCO_2 is lowered.

It should be noted that Na removal acidified the cells on the order of 0.5 pH units (Tables IV and V). No late alkalization was observed as described for the rabbit S_3 segment (27) or the rat PCT (28, 29). In all other protocols, baseline cell pH values were not significantly different in control and experimental periods.

Discussion

Relative roles of ambient pH, HCO_3 and PCO_2 as determinants of cell pH. When ambient pH was changed, the resultant cell pH change was not statistically different whether ambient pH was changed by varying extracellular $[\text{HCO}_3]$ or PCO_2 (Table II). All cell pH changes were in the same direction but smaller than the imposed extracellular pH change. When PCO_2 and $[\text{HCO}_3]$ were changed simultaneously such that pH was constant (isohydric changes), cell pH did not change significantly (Table III). These findings are consistent with the observation in the rabbit PCT that ambient pH is the main regulator of HCO_3 reabsorption (5) and phenomenologically suggest that ambient pH is the main determinant of cell pH.

Table IV. Cell pH Defense to an Acute Increase in PCO_2 from 40 to 105 mmHg/ pH_e^* (7.4 to 7.0)

| | Baseline pH | ΔpH_i , initial | ΔpH_i , steady state | Cell pH defense $d\text{pH}_i/dt$ | Number of tubules |
|---------------------|-------------------------|-------------------------------|------------------------------------|--------------------------------------|-------------------|
| C(+Na) [‡] | 7.31±0.05 | 0.33±0.04 | 0.23±0.03 | +0.17±0.04 | 6 |
| E(-Na) [§] | 6.72±0.05 | 0.13±0.01 | 0.13±0.02 | +0.01±0.01 | |
| C(+Cl) | 7.27±0.03 | 0.34±0.04 | 0.24±0.04 | +0.13±0.03 | 8 |
| E(-Cl) | 7.28±0.07 (NS) | 0.35±0.03 (NS) | 0.26±0.03 (NS) | +0.16±0.02 (NS) | |
| C(-SITS) | 7.35±0.02 | 0.32±0.02 | 0.22±0.02 | +0.20±0.05 | 6 |
| E(+SITS) | 7.30±0.03 (NS) | 0.29±0.01 (NS) | 0.20±0.03 (NS) | +0.06±0.02 [†] | |
| C(-amiloride) | 7.33±0.02 | 0.30±0.02 | 0.19±0.03 | +0.21±0.06 | 5 |
| E(+amiloride) | 7.36±0.03 (NS) | 0.33±0.02 (NS) | 0.28±0.04 [†] | +0.06±0.04 ^{**} | |

* pH_e , external (ambient) pH. ‡ C, control. § E, experimental. || $P < 0.001$ compared with control. † $P < 0.01$ compared with control.

** $P < 0.025$ compared with control.

Table V. Cell pH Response to an Acute Decrease in PCO₂ from 40 to 10 mmHg (pH_e* 7.4 to 8.0)

| | Baseline pH | ΔpH _i , initial | ΔpH _i , steady state | Cell pH defense <i>dpH_i/dt</i> | Number of tubules |
|---------------------|-------------------------|----------------------------|---------------------------------|--|-------------------|
| C(+Na) [‡] | 7.35±0.04 | 0.43±0.02 | 0.34±0.04 | -0.16±0.06 | 5 |
| E(-Na) [§] | 6.91±0.02 | 0.21±0.02 | 0.23±0.04 [†] | +0.01±0.02 | |
| C(+Cl) | 7.38±0.03 | 0.43±0.02 | 0.35±0.03 | -0.31±0.06 | 9 |
| E(-Cl) | 7.34±0.03 (NS) | 0.43±0.03 (NS) | 0.30±0.04 (NS) | -0.29±0.06 (NS) | |
| C(-SITS) | 7.27±0.04 | 0.44±0.03 | 0.30±0.03 | -0.13±0.02 | 6 |
| E(+SITS) | 7.27±0.04 (NS) | 0.40±0.01 (NS) | 0.31±0.05 (NS) | -0.03±0.02 | |
| C(-Amiloride) | 7.33±0.02 | 0.39±0.02 | 0.33±0.03 | -0.26±0.05 | 5 |
| E(+Amiloride) | 7.39±0.06 (NS) | 0.42±0.03 (NS) | 0.35±0.05 (NS) | -0.20±0.04 (NS) | |

* pH_e, external (ambient) pH. ‡ C, control. § E, experimental. || P < 0.001 compared with control. † P < 0.005 compared with control.

However, the correlation of steady-state cell pH with extracellular fluid pH is also consistent with separate effects of extracellular [HCO₃] or PCO₂ which are of similar magnitude. In fact, based on our understanding of the mechanisms involved, this explanation is more likely. The major effect of ambient [HCO₃] on cell pH is via the SITS-sensitive basolateral membrane Na/(HCO₃)₃ transporter (Figs. 2 and 3, reference 26). While this transporter may be pH sensitive, previous studies demonstrated that HCO₃ is the substrate transported (13, 16, 17, 30) and thus is most likely the key rate determinant. PCO₂ affects cell pH in a more complex manner which involves CO₂ diffusion into cells, titration of cellular buffers, and defense of cell pH by Na-coupled apical and basolateral membrane transporters. Changes in extracellular pH may contribute. Therefore, given the complexities of cell pH responses to changes in ambient [HCO₃] or PCO₂, these responses cannot be considered to occur by the same mechanism, regulated by ambient pH, although they are similar in magnitude.

For [HCO₃] changes at constant PCO₂ the ratio of ΔpH_i/ΔpH_e was 0.67 and therefore higher than that of 0.31 reported for canine proximal tubule cells using 5,5-dimethyl-2,4-oxazolidinedione as a measure of cell pH (31). This discrepancy may be due to species differences, to the inability to change luminal [HCO₃] in cell suspensions, or to technical problems with 5,5-dimethyl-2,4-oxazolidinedione (32). Our ratio for ΔpH_i/ΔpH_e of 0.64 for changes in PCO₂ while [HCO₃] was held constant is similar to the value of 0.58 in canine proximal tubule cells (31) and is also in close agreement with the value of 0.67 reported for the rat PCT in vivo (29).

Relative roles of luminal and peritubular membrane HCO₃/OH/H transporters as determinants of cell pH. A comparison of the ratio of ΔpH_i/ΔpH_e when [HCO₃] was changed symmetrically (0.67, Fig. 1) with our previous results, which showed a ΔpH_i/ΔpH_e of 0.5 when only peritubular [HCO₃] was changed (17), suggests a predominant control of cell pH by the rate of the basolateral membrane transporters, as also

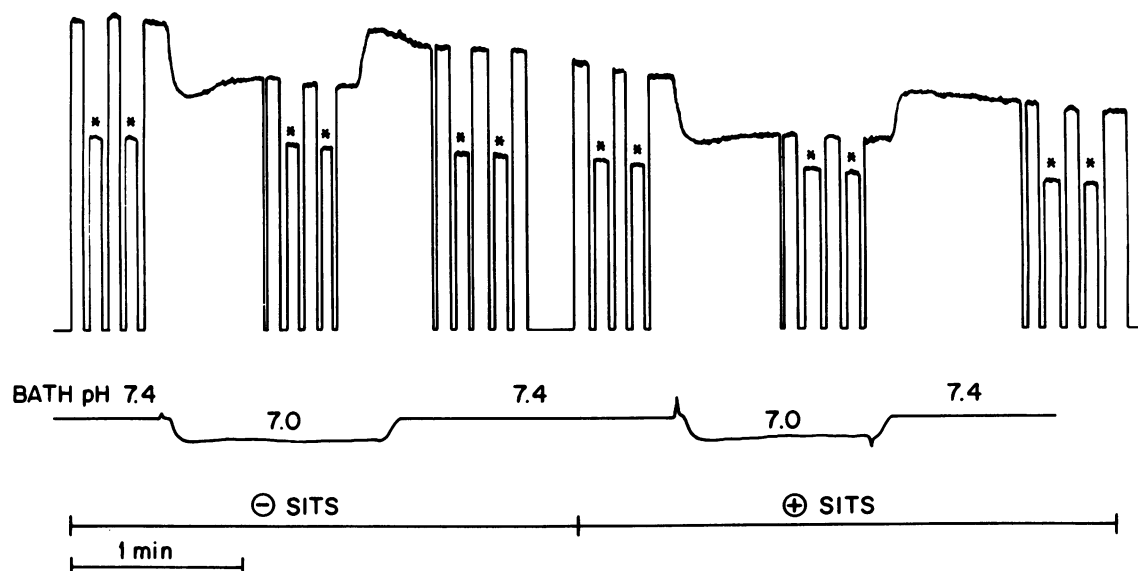


Figure 5. Effect of 1 mM bath SITS on the cell pH response to an increase in PCO₂ from 40 to 105 mmHg: original study. In the absence of bath SITS, the 500-nm fluorescence increases slowly to reach a new steady state reflecting cell pH defense. In the presence of bath SITS the increase in 500-nm fluorescence and thus cell pH recovery is inhibited.

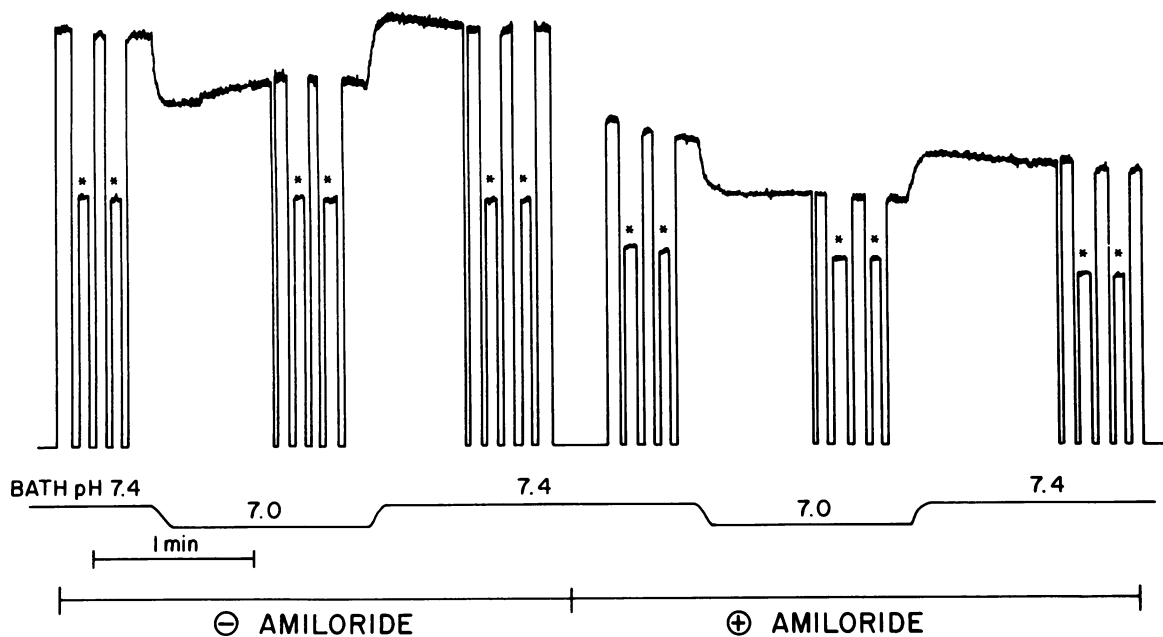


Figure 6. Effect of 1 mM luminal amiloride on the cell pH response to an increase in PCO_2 from 40 to 105 mmHg: original study. The increase in 500-nm fluorescence during the recovery period (cell pH defense, left tracing) is inhibited by amiloride (right tracing).

found by Alpern and Chambers in the rat PCT (26). In agreement, we found that a decrease in luminal $[HCO_3^-]$ from 25 to 6.25 (luminal pH change of -0.6 pH units) decreased cell pH by only 0.05 pH units (Fig. 2), while an increase in luminal $[HCO_3^-]$ from 25 to 95 mM (luminal pH change of $+0.6$ pH units) increased cell pH by 0.04 pH units (Fig. 3). These small changes in cell pH could be explained assuming that a decrease in luminal pH would slow the apical Na/H antiporter, which would acidify the cells. Cell acidification, however would be expected to inhibit the basolateral Na/(HCO₃)₃ cotransporter, which would attenuate the cell pH change. The reverse would be true when luminal $[HCO_3^-]$ is raised. In support of this, in the presence of inhibition of the basolateral Na/(HCO₃)₃ cotransporter, changes in luminal $[HCO_3^-]$ induced much larger cell pH changes (Figs. 2 and 3). Thus, in the rabbit PCT, cell pH is primarily determined by the activity of the basolateral Na/(HCO₃)₃ cotransporter, and peritubular pH and $[HCO_3^-]$

by changing the rate of this transporter are more important in setting steady state cell pH than are luminal pH and $[HCO_3^-]$.

Changes in peritubular pH and $[HCO_3^-]$ affect the rate of the Na/(HCO₃)₃ cotransporter, and secondarily have profound effects on cell pH. Cell pH then alters apical Na/H antiport by altering its driving forces and, in addition, by allosteric regulation (33). By changing the rate of the apical Na/H antiporter increases or decreases in luminal $[HCO_3^-]$ lead to changes in cell pH (and cell Na concentration), which secondarily increase or decrease, respectively, the rate of the basolateral Na/(HCO₃)₃ cotransporter. The net effect of these events would then be altered transcellular proton secretion or HCO₃ reabsorption at the expense of a change in cell pH. These results explain the marked sensitivity of the proton secretory rate to luminal and peritubular $[HCO_3^-]$ (2, 5).

Determinants of cell pH response to acute changes in PCO_2 ("cell pH defense"). The typical cell pH response to an acute change in ambient PCO_2 is illustrated and explained in Fig. 4. When ambient PCO_2 is acutely changed there is a sudden change in cell PCO_2 which is equal in magnitude. The failure of cell pH to initially change as much as extracellular pH is due to the chemical buffering by the nonbicarbonate buffers of the cell. Thus, the magnitude of the early cell pH response reflects the nonbicarbonate buffering power of the cell, which can be calculated from the immediate changes in cell pH both for increases of PCO_2 from 40 to 105 mm Hg and decreases from

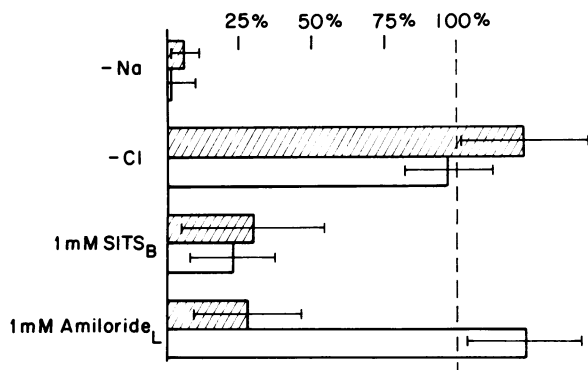


Figure 7. Cell pH defense in response to acute changes in PCO_2 (open bars) PCO_2 changed from 40 to 10 mmHg; (stippled bars) PCO_2 changed 40 to 105 mmHg. The values represent the cell pH recovery (dpH_i/dt) in percentage of controls.

3. An acute influx or efflux of CO_2 increases or decreases H^+ and $[HCO_3^-]$ in the cell. Most of the changes in H^+ concentration are buffered by binding or release of H^+ by non- CO_2 cellular buffers. Since for each HCO₃ formed or consumed one H⁺ is released or bound, respectively, the non- CO_2 buffer capacity, B_1 , is given by the formula:

$$B_1 = -\Delta[HCO_3^-]_i / \Delta pH_i, \quad (1)$$

where $[HCO_3^-]_i$ can be calculated according to:

$$[HCO_3^-]_i = 0.03 \cdot PCO_2 \cdot 10^{pH_i - pK}, \quad (2)$$

40 to 10 mmHg.³ The nonbicarbonate buffering power was 18.3 ± 2.3 mmol/liter · pH unit when PCO_2 was increased and 16.8 ± 2.4 mmol/liter · pH unit when PCO_2 was decreased (NS). The total buffer capacity is obtained when the buffering power of intracellular $[HCO_3^-]/CO_2$ is added. The total buffer capacity calculated when using increases in PCO_2 was 62.2 ± 7.4 mmol/liter · pH unit and when using decreases in PCO_2 was 60.4 ± 9.3 mmol/liter · pH unit (NS, $n = 8$). These values are lower than our previously reported buffer capacity using another method (rapid NH_3 washout) of 84.6 ± 7.3 mmol/liter · pH unit in the presence of ambient PCO_2 (total buffering power) and 42.8 ± 5.6 in the absence of exogenous CO_2 (approximating nonbicarbonate buffering power, [17]). The reason(s) for these differences are unclear.⁴

Our studies show that cell pH recovery from an acute decrease in PCO_2 (from 40 to 10 mmHg, ambient pH change from 7.4 to 8.0) is sodium-dependent and chloride-independent and is inhibited by peritubular SITS, while luminal amiloride has no effect (Table V, Fig. 7). Cell pH recovery from an acute increase in PCO_2 (from 40 to 105 mmHg, ambient pH change from 7.4 to 7.0) is also sodium-dependent and chloride-independent. Recovery can be blocked, however, both by luminal amiloride and peritubular SITS (Table IV, Figs. 5–7).

Defense of intracellular pH could be effected by apical (35–38) and basolateral (28, 39, 40) Cl/base exchangers. Chloride-dependence of the cell response to an acute alkaline (but not acid) load has been described in leukocytes (41). In addition, in canine proximal tubule cells, recovery from an alkaline load (induced by NH_3) has been found to be chloride-dependent (42). Our results demonstrate, however, that the contribution of Cl/base exchange mechanisms to cell pH defense in response to acute changes in PCO_2 is small or nonexistent in the rabbit PCT (Tables IV and V). The lack of importance of chloride-coupled transporters in cell pH regulation agrees with

and ΔpH_i is measured directly. B_{CO_2} , the buffer capacity of CO_2/HCO_3^- , can be calculated according to the formula (34):

$$B_{CO_2} = 2.3 [HCO_3^-]_i \quad (3)$$

Hence, the total buffer capacity, B_T , is given by:

$$B_T = B_i + B_{CO_2} \quad (4)$$

It should be noted that the buffer capacity was determined without inhibition of cell pH defense (e.g., luminal amiloride, bath SITS). In view of the fact that the rates of cell pH defense were on the order of 0.1–0.2 pH units min^{-1} and the rates of cell pH change after sudden changes of PCO_2 were above 5 pH units min^{-1} , failure to inhibit cell pH defense should not have affected the estimates of buffering power significantly.

4. The differences may be due in part to the fact that the previous results were obtained using solutions buffered with Hepes. If Hepes enters the cells, it could contribute to the nonbicarbonate buffer capacity. When the buffer capacity was estimated (NH_3 washout, 1 mM amiloride in lumen and 1 mM SITS in the bath fluid to minimize cell pH defense) in the same tubule using HCO_3^- -buffered solution with and without addition of HEPES (25 mM), we found that addition of Hepes increased our estimate of buffer capacity by ~ 8 –10 mmol/liter · pH unit ($n = 4$). These preliminary observations and the permeability of Hepes into proximal tubule cells need further studies. Metabolic production of HCO_3^- is unlikely to have contributed significantly to the buffer capacity determined in our previous study. The intracellular $[HCO_3^-]$ produced by metabolism is probably < 0.4 mM (17). Thus, the contribution of metabolically produced HCO_3^- to the buffer capacity would be at most 1 mmol/liter · pH unit.

previous studies which have found that chloride removal does not affect the rate of bicarbonate absorption in the rabbit PCT and PST (43–45).

The sodium dependence, along with the SITS and amiloride sensitivity of the cell pH defense, demonstrate an important role for the Na/H antiporter and the $Na/(HCO_3)_3$ symporter. This latter transport system defends cell pH in response to both increases and decreases in PCO_2 . The lack of effect of amiloride on the cell pH response to a decrease in PCO_2 suggests that changes in Na/H antiporter rate are quantitatively less important in this setting. Because of the low intracellular Na concentration, the antiporter may be expected to transport protons out of the cell even when PCO_2 is decreased. However, the increase in cell pH could slow the antiporter rate by allosteric (down)regulation (33). Therefore, further inhibition of the transporter by amiloride may be undetectable.

In conclusion, our studies demonstrate that (a) ambient $[HCO_3^-]$ and PCO_2 have quantitatively similar effects on cell pH in the rabbit PCT; (b) the basolateral $Na/(HCO_3)_3$ cotransporter is a more important determinant of cell pH than the luminal $HCO_3^-/OH^-/H$ membrane transport processes; (c) cell pH response to acute changes in PCO_2 is primarily dependent on the basolateral $Na/(HCO_3)_3$ cotransporter (acid and alkaline loads) and the luminal Na/H antiporter (acid loads), while Cl/base exchange processes do not contribute significantly.

Acknowledgments

The able secretarial help of Gracie Bernacki is gratefully acknowledged.

This study was supported by grants DK-27945 and DK-26142 from the National Institutes of Health. Dr. Krapf is the recipient of a generous grant from the Swiss National Foundation. Dr. Alpern is the recipient of a Clinical Investigator Award, DK-01229.

References

1. Alpern, R. J., D. G. Warnock, and F. C. Rector, Jr. 1986. Renal acidification mechanisms. In B. M. Brenner, and F. C. Rector, Jr., editors. The Kidney. 3rd edition. W. B. Saunders Co., Philadelphia.
2. Alpern, R. J., M. G. Cogan, and F. C. Rector, Jr. 1982. Effect of luminal bicarbonate concentration on proximal acidification in the rat. *Am. J. Physiol.* 243 (Renal Fluid Electrolyte Physiol. 12):F53–F59.
3. Malnic, G., and M. de Mello-Aires. 1971. Kinetic study of bicarbonate reabsorption in proximal tubule of the rat. *Am. J. Physiol.* 220:1759–1767.
4. Ullrich, K. J., G. Rumrich, and K. Baumann. 1975. Renal proximal tubular buffer-(glycodiazine) transport. *Pfluegers Arch. Eur. J. Physiol.* 357:149–163.
5. Sasaki, S., C. A. Berry, and F. C. Rector, Jr. 1982. Effect of luminal and peritubular HCO_3^- concentrations and PCO_2 on HCO_3^- reabsorption in rabbit proximal convoluted tubules perfused in vitro. *J. Clin. Invest.* 70:639–649.
6. Aronson, P. S., M. A. Suhm, and J. Nee. 1983. Interaction of external H^+ with Na^+-H^+ exchanger in renal microvillus membrane vesicles. *J. Biol. Chem.* 258:6767–6771.
7. Alpern, R. J., M. G. Cogan, and F. C. Rector, Jr. 1983. Effects of extracellular fluid volume and plasma bicarbonate concentration on proximal acidification in the rat. *J. Clin. Invest.* 71:736–746.
8. Chan, Y. L., B. Biagi, and G. Giebisch. 1982. Control mechanisms of bicarbonate transport across the rat proximal convoluted tubule. *Am. J. Physiol.* 242 (Renal Fluid Electrolyte Physiol. 11):F532–F543.

9. Giebisch, G., G. Malnic, G. B. de Mello, and D. de Mello-Aires. 1977. Kinetics of luminal acidification in cortical tubules of the rat kidney. *J. Physiol. (Lond.)* 267:571-599.
10. Kunau, R. T., J. I. Hart, and K. A. Walker. 1985. Effect of metabolic acidosis on proximal tubular tCO₂ absorption. *Am. J. Physiol.* 249 (Renal Fluid Electrolyte Physiol. 18):F62-F68.
11. Mello-Aires, M., and G. Malnic. 1975. Peritubular pH and PCO₂ in renal tubular acidification. *Am. J. Physiol.* 228:1766-1774.
12. Boron, W. F., and E. L. Boulpaep. 1983. Intracellular pH regulation in the renal proximal tubule of the salamander: basolateral HCO₃⁻ transport. *J. Gen. Physiol.* 81:53-94.
13. Akiba, T., R. J. Alpern, J. Eveloff, J. Calamina, and D. G. Warnock. 1986. Electrogenic sodium bicarbonate cotransport in rabbit renal cortical basolateral membrane vesicles. *J. Clin. Invest.* 78:1472-1478.
14. Alpern, R. J. 1985. Mechanism of basolateral membrane H⁺/OH⁻/HCO₃⁻ transport in the rat proximal convoluted tubule: a sodium-coupled electrogenic process. *J. Gen. Physiol.* 86:613-637.
15. Biagi, B. A., and M. Sohtell. 1986. Electrophysiology of basolateral bicarbonate transport in the rabbit proximal tubule. *Am. J. Physiol.* 250 (Renal Fluid Electrolyte Physiol. 19):F267-F272.
16. Grassl, S. M., and P. S. Aronson. 1986. Na⁺/HCO₃⁻ cotransport in basolateral membrane vesicles isolated from rabbit renal cortex. *J. Biol. Chem.* 261:8778-8783.
17. Krapf, R., R. J. Alpern, F. C. Rector, Jr., and C. A. Berry. 1987. Basolateral membrane Na/base cotransport is dependent on CO₂/HCO₃⁻ in the proximal convoluted tubule. *J. Gen. Physiol.* In press.
18. Sasaki, S., T. Shiiga, N. Yoshiyama, and J. Takeuchi. 1987. Mechanism of bicarbonate exit across basolateral membrane of the rabbit proximal straight tubule: a microelectrode study. *Am. J. Physiol.* 252 (Renal Fluid Electrolyte Physiol. 21):F11-F18.
19. Soleimani, M., S. M. Grassl, and P. S. Aronson. 1987. Stoichiometry of Na/HCO₃⁻ cotransport in basolateral membrane vesicles isolated from rabbit renal cortex. *J. Clin. Invest.* 79:1276-1280.
20. Cogan, M. G. 1984. Effects of acute alterations in PCO₂ on proximal HCO₃⁻, Cl⁻, and H₂O reabsorption. *Am. J. Physiol.* 246 (Renal Fluid Electrolyte Physiol. 15):F21-F26.
21. Jacobson, H. R. 1981. Effects of CO₂ and acetazolamide on bicarbonate and fluid transport in rabbit proximal tubules. *Am. J. Physiol.* 240 (Renal Fluid Electrolyte Physiol. 9):F54-F62.
22. Levine, D. Z. 1971. Effect of acute hypercapnia on proximal tubular water and bicarbonate absorption. *Am. J. Physiol.* 221:1164-1170.
23. Burg, M. B., J. Grantham, M. Abramow, and J. Orloff. 1966. Preparation and study of fragments of the single rabbit nephron. *Am. J. Physiol.* 210:1293-1298.
24. Thomas, J. A., R. N. Buchsbaum, A. Zimnick, and F. Racke. 1979. Intracellular pH measurements in Ehrlich ascites tumor cells utilizing spectroscopic probes generated in situ. *Biochemistry.* 18:2210-2218.
25. Schwartz, G. J., A. M. Weinstein, R. E. Steele, J. L. Stephenson, and M. B. Burg. 1981. Carbon dioxide permeability of rabbit proximal convoluted tubules. *Am. J. Physiol.* 240 (Renal Fluid Electrolyte Physiol. 9):F231-F244.
26. Alpern, R. J., and M. Chambers. 1986. Cell pH in the rat proximal convoluted tubule. Regulation by luminal and peritubular pH and sodium concentration. *J. Clin. Invest.* 78:502-510.
27. Nakhoul, N. L., and W. F. Boron. 1985. Intracellular pH regulation in rabbit proximal straight tubules: dependence on external sodium. *Fed. Proc.* 44:1898. (Abstr.)
28. Alpern, R. J., and M. Chambers. 1987. Basolateral membrane Cl/HCO₃⁻ exchange in the rat proximal convoluted tubule: Na-dependent and independent modes. *J. Gen. Physiol.* 87:581-598.
29. Yoshitomi, K., B.-Ch. Buckhardt, and E. Froemter. 1985. Rheogenic sodium-bicarbonate cotransport in the peritubular cell membrane of rat renal proximal tubule. *Pfluegers Arch. Eur. J. Physiol.* 405:360-366.
30. Soleimani, M., and P. S. Aronson. 1987. Effect of acetazolamide on the Na⁺/HCO₃⁻ cotransport in renal basolateral membrane vesicles. *Kidney Int.* 31:416. (Abstr.)
31. Struyvenberg, A., R. B. Morrison, and A. S. Relman. 1968. Acid-base behavior of separated canine renal tubule cells. *Am. J. Physiol.* 214:1155-1162.
32. Adler, S., A. Roy, and A. S. Relman. 1965. Intracellular acid-base regulation. I. The response of muscle cells to changes in CO₂ tension or extracellular bicarbonate concentration. *J. Clin. Invest.* 44:8-20.
33. Aronson, P. S., J. Nee, and M. A. Suhm. 1982. Modifier role of internal H⁺ in activating the Na⁺-H⁺ exchanger in renal microvillus membrane vesicles. *Nature (Lond.)* 299:161-163.
34. Roos A., and W. F. Boron. 1981. Intracellular pH. *Physiol. Rev.* 61:296-434.
35. Karniski, L. P., and P. S. Aronson. 1985. Chloride/formate exchange with formic acid recycling: A mechanism of active chloride transport across epithelial membranes. *Proc. Natl. Acad. Sci. USA.* 82:6362-6365.
36. Alpern, R. J. 1987. Apical membrane Cl/base exchange in the rat proximal convoluted tubule. *J. Clin. Invest.* 79:1026-1030.
37. Baum, M. 1987. Evidence that parallel Na⁺/H⁺ and Cl⁻/HCO₃⁻(OH⁻) antiporters transport NaCl in the rabbit proximal convoluted tubule. *Am. J. Physiol.* 252 (Renal Fluid Electrolyte Physiol. 21):F338-F345.
38. Lucci, M. S., and D. G. Warnock. 1979. Effects of anion transport inhibitors on NaCl reabsorption in the rat superficial proximal convoluted tubule. *J. Clin. Invest.* 64:570-579.
39. Grassl, S. M., L. P. Karniski, and P. S. Aronson. 1985. Cl-HCO₃⁻ exchange in rabbit renal cortical basolateral membrane vesicles (BLMV). *Kidney Int.* 27:282. (Abstr.)
40. Sasaki, S., K. Ishibashi, N. Yoshiyama, T. Shiigai, and J. Takeuchi. 1987. Cl/HCO₃⁻ exchange at basolateral membrane of rabbit proximal tubule. *Kidney Int.* 31:415. (Abstr.)
41. Simchowitz, L., and A. Roos. 1985. Regulation of intracellular pH in human neutrophils. *J. Gen. Physiol.* 85:443-470.
42. Reid, I. R., R. Civitelli, S. L. Westbrook, L. V. Avioli, and K. A. Hruska. 1987. Cytoplasmic pH regulation in canine renal proximal tubular cells. *Kidney Int.* 31:1113-1120.
43. Burg, M. B., and N. Green. 1977. Bicarbonate transport by isolated perfused rabbit proximal convoluted tubules. *Am. J. Physiol.* 233 (Renal Fluid Electrolyte Physiol. 2):F307-F314.
44. McKinney, T. D., and M. Burg. 1977. Bicarbonate and fluid absorption by renal proximal straight tubules. *Kidney Int.* 12:1-8.
45. Sasaki, S., and C. A. Berry. 1984. Mechanism of bicarbonate exit across basolateral membrane of the rabbit proximal convoluted tubule. *Am. J. Physiol.* 246 (Renal Fluid Electrolyte Physiol. 15):F889-F896.